Clinical and Experimental Medicine (2025) 25:200
https://doi.org/10.1007/s10238-025-01745-5

RESEARCH

Exploring the molecular mechanisms of lactylation-related biological functions and immune regulation in sepsis-associated acute kidney injury

Kui Jiang[1] · Shujuan Mai[2] · Jian Li[1] · Hongxing Zhou[1] · Yu Chen[1] · Leyuan Zou[1] · Huixia Yu[1]

Received: 19 February 2025 / Accepted: 21 May 2025
© The Author(s) 2025

Abstract

Lactylation, a novel post-translational modification, has been implicated in various pathophysiological processes; however, its role in sepsis-associated acute kidney injury (SA-AKI) remains unclear. This study aimed to investigate the expression patterns and potential functional roles of lactylation-related genes (LRGs) in SA-AKI using transcriptomic data from the GSE232404 dataset. A total of 118 differentially expressed LRGs were identified, enriched in pathways related to RNA splicing, histone deacetylation, and carbon metabolism pathways. Immune infiltration analysis revealed significant alterations in macrophages M0, neutrophils, and T cell subtypes. Consensus clustering-based molecular subtyping stratified SA-AKI samples into two distinct clusters, each characterized by unique immune landscapes and enrichment in cytokine signaling pathways. Weighted gene co-expression network analysis (WGCNA) identified the darkseagreen3 module as highly correlated with these subtypes. Subsequent machine learning analyses, incorporating Lasso regression and random forest algorithms, identified *PECR* and *TP53I3* as key LRGs. Transcription factor enrichment analysis further suggested motif cisbp__M1413 as a potential upstream regulator. Single-cell RNA sequencing (scRNA-seq) analysis revealed *PECR* and *TP53I3* were predominant expression in proximal tubule and Loop of Henle cells, with significant correlations to lactylation-related pathways. This comprehensive analysis finds the potential roles of LRGs in SA-AKI pathogenesis, particularly their association with immune regulation and cell-type specificity. The identified of *PECR* and *TP53I3* provides new insights into the molecular mechanisms of SA-AKI and may inform the development of targeted therapeutic strategies.

Keywords SA-AKI · Lactylation · Subtype analysis · Immune regulation · scRNA-seq · SA-AKI biomarkers

Introduction

SA-AKI is a complex and high-risk clinical condition that presents substantial challenges in treatment and management [1, 2]. Currently, the therapeutic strategies primarily focus on controlling the underlying cause, preserving renal function and preventing further kidney injury. Clinical interventions include optimizing hemodynamic stability through appropriate fluid management and vasopressor support to enhance renal perfusion, maintaining strict glycemic control to avoid tubular cell injury caused by hyperglycemia or hypoglycemia; and regulating lipid levels to minimize vascular endothelial injury [3]. Additionally, nephrotoxic drugs, such as certain antibiotics and non-steroidal anti-inflammatory drugs, should be avoided [4]. Effective fluid management is crucial to prevent both fluid overload, which can cause interstitial edema, and hypovolemia, which compromises renal perfusion. Nutritional support, including moderate protein intake and a balanced diet, may help reduce the renal burden. Targeted therapies such as antioxidants can alleviate oxidative stress by scavenging reactive oxygen species, while immunomodulators and anti-inflammatory agents may suppress excessive immune and inflammatory responses [5, 6]. For patients with severe SA-AKI, renal

Kui Jiang, Shujuan Mai, and Jian Li have contributed equally to this work.

✉ Leyuan Zou
531362457@qq.com

✉ Huixia Yu
slobberfish@163.com

[1] Department of Nephrology, The First Affiliated Hospital of Jinan University, Guangzhou, Guangdong Province, China

[2] Intensive Care Unit, The First Affiliated Hospital of Jinan University, Guangzhou, Guangdong Province, China

Published online: 12 June 2025

replacement therapy (RRT) plays a vital role in removing toxins, maintaining fluid and electrolyte balance, and correcting acid–base disturbances [7]. Prognosis management requires regular monitoring of renal biomarkers, including serum creatinine, blood urea nitrogen, and urinary clearance, is essential for early detection and intervention of renal function decline. Lifestyle modifications, including smoking cessation, alcohol limitation, moderate exercise, and weight control, are essential for slowing disease progression. Ultimately, individualized treatment plans and multidisciplinary collaboration, particularly for critically ill patients, are crucial for improving the long-term outcomes of SA-AKI [8].

SA-AKI is a common and severe complication of sepsis, characterized by complex pathological mechanisms including oxidative stress, inflammatory responses, and apoptosis [9, 10]. Oxidative stress in SA-AKI is driven by excessive production of reactive oxygen species (ROS) and peroxides, which disrupt the lipid bilayer structure of cell membranes and damage DNA and proteins. Additionally, dysfunction of antioxidant enzymes, such as superoxide dismutase and glutathione peroxidase exacerbates oxidative injury [11]. Inflammatory responses are marked by the overactivation of immune cells, including macrophages, monocytes, and lymphocytes, leading to the release of inflammatory mediators, such as tumor necrosis factor-alpha (TNF-α), interleukin-6 (IL-6), and interleukin-1β (IL-1β). This leads to a cascade of inflammatory responses, resulting in both local and systemic tissue injury [12, 13]. In addition, Sepsis also promotes renal tubular epithelial cell apoptosis via caspase-dependent and -independent pathways, further impairing renal function [14, 15]. Epidemiological studies indicate that the incidence of SA-AKI exceeds 50% among critically ill patients in intensive care units [16], with risk factors including hypertension, diabetes, hyperlipidemia, chronic infections, drug toxicity, and advanced age or multi-organ dysfunction syndrome (MODS) [3, 17].-Despite extensive research into its mechanisms, SA-AKI remains a major clinical challenge. A deeper understanding of its pathogenesis and risk factor–targeted interventions is critical to improving outcomes.

The rapid development of bioinformatics has provided powerful tools for exploring the pathogenesis of complex diseases and identifying potential therapeutic targets. Among high-throughput platforms, gene microarray technology enables comprehensive profiling of gene expression, offering molecular insights into disease pathophysiology [18]. In SA-AKI, bioinformatics analyses have been extensively applied to analyze microarray data, identify key biomarkers, and reveal relevant signaling pathways [19, 20]. For instance, gene microarray technology has uncovered numerous genes implicated in inflammation, oxidative stress, and apoptosis, with subsequent validation studies clarifying their regulatory networks and roles in disease progression. Beyond transcriptomic analysis, the scope of bioinformatics now encompasses proteomics, metabolomics, and non-coding RNA studies, allowing for a systems-level understanding of disease mechanisms. Integration of multi-omics data facilitates the construction of more precise disease network models and supports the development of personalized treatment strategies and targeted drug discovery [21]. The combination of gene microarray and bioinformatics has become an essential approach for uncovering the mechanisms of complex diseases and optimizing therapeutic decision-making [22].

Lactylation, a recently discovered post-translational modification, involves the addition of a lactyl group to lysine residues of proteins, and it has been shown to regulate immune responses. In inflammatory conditions such as sepsis, which is closely related to SA-AKI, metabolic reprogramming occurs, including the upregulation of glycolysis and lactate production [23]. This shift in metabolism can lead to increased lactate accumulation, which may subsequently influence protein lactylation. Lactylation has been shown to modulate the function of immune cells, such as macrophages and T cells, potentially impacting inflammatory responses [24, 25]. Given the central role of inflammation in SA-AKI pathogenesis, lactylation offers a promising mechanism for modulating immune function and inflammation. Lactylation is also closely linked to cellular stress responses. Under conditions of oxidative stress and metabolic dysregulation, such as those seen in sepsis and acute kidney injury, lactylation may play a role in adapting cellular function to stress. Mitochondrial dysfunction is a key feature of SA-AKI, and lactylation has been implicated in regulating mitochondrial function. Lactylation can influence mitochondrial proteins, potentially altering mitochondrial metabolism and function [23]. Given these mechanisms, we believe that lactylation may be a novel and important post-translational modification in the context of SA-AKI, with potential implications for immune modulation, cellular stress responses, and mitochondrial function.

In this study, single-cell sequencing combined with bulk transcriptome analysis was used to compare expression profiles between patients with SA-AKI injury and healthy controls. LRGs were analyzed to classify molecular subtypes of the disease group, exploring immune cell infiltration and functional enrichment among different subtypes. Key genes were identified using weighted gene co-expression network analysis(WGCNA) networks and machine learning approaches. These findings enhance our understanding of the molecular mechanisms of SA-AKI and provide a foundation for the development of novel diagnostic biomarkers and targeted therapies. The overall analysis workflow is presented in Supplementary Fig. 1.

Materials and methods

Data download

The Gene Expression Omnibus (GEO) database (https://www.ncbi.nlm.nih.gov/geo /info/datasets.html) is a comprehensive repository for gene expression data, developed and maintained by the National Center for Biotechnology Information (NCBI). For this study, the Series Matrix File of dataset GSE232404 was retrieved from the GEO database, encompassing expression profile data from a total of 10 patients, including 5 from the control group and 5 from the disease group. Additionally, single-cell expression data from dataset GSE174220 were downloaded, selecting samples from 2 cases with complete expression profiles for subsequent analysis.

Functional enrichment analysis

To elucidate the biological functions and signaling pathways associated with the gene set, the R package ClusterProfiler was employed for functional annotation, enabling a comprehensive exploration of the functional relevance of these genes. Gene Ontology (GO) and Kyoto Encyclopedia of Genes and Genomes (KEGG) analyses were performed to identify relevant functional categories and pathways. Pathways enriched in GO and KEGG analyses with both a p-value and q-value less than 0.05 were considered statistically significant.

Immune cell infiltration analysis

The CIBERSORT method is a widely utilized tool for evaluating immune cell types within the tumor microenvironment. Based on support vector regression, this method performs deconvolution analysis on the expression matrix of immune cell subtypes. It includes 547 biomarkers that distinguish 22 human immune cell phenotypes, encompassing various T cell, B cell, plasma cell, and myeloid cell subsets. In this study, the CIBERSORT algorithm was employed to analyze patient data, enabling the estimation of the relative proportions of 22 immune infiltrating cell types. A subsequent correlation analysis was conducted to assess the relationship between gene expression and immune cell composition.

Consensus clustering molecular typing

Based on the expression profiles of key LRGs, a consistent clustering method was employed to group the septic kidney injury samples. A total of 50 iterations were performed for clustering, with each iteration including 80% of the samples. The optimal number of clusters was determined by analyzing the cumulative distribution function curve of the consistency score, along with the characteristics observed in the consistency matrix heatmap.

Differential expression analysis

The Limma package is an R software tool commonly used for differential expression analysis of gene expression profiles, enabling the identification of significantly differentially expressed genes between groups. In this study, the Limma package was utilized to analyze the molecular mechanisms underlying septic kidney injury, identifying differentially expressed genes between sample types. Differentially expressed genes were selected based on the criteria of an adjusted p-value (adj.P.Val) < 0.05 and $|\log FC| > 2$. Subsequently, volcano plots and heatmaps were generated to visualize the differential gene expression.

WGCNA analysis

By constructing a weighted gene co-expression network, we can identify co-expressed gene modules, investigate the correlation between gene networks and diseases, and highlight key genes within the network. The WGCNA R package was employed to construct a co-expression network for all genes in the dataset. Genes exhibiting the top 10,000 variances were selected for further analysis. The soft threshold was set to 21. The weighted adjacency matrix was then transformed into a topological overlap matrix (TOM) to assess network connectivity, and hierarchical clustering was applied to construct the clustering dendrogram of the TOM matrix. Different branches of the dendrogram represent distinct gene modules, with various colors indicating separate modules. Genes were classified based on their expression patterns using the weighted correlation coefficient, with genes sharing similar expression profiles grouped into individual modules. Ultimately, all genes were classified into multiple modules based on their expression patterns.

Machine learning algorithm identifies key genes

To identify key diagnostic genes associated with SA-AKI, we applied two complementary machine learning approaches: Least Absolute Shrinkage and Selection Operator (LASSO) regression and the random forest (RF) algorithm. LASSO was used to reduce model complexity and select the most informative features by penalizing the absolute size of the regression coefficients. In parallel, the RF algorithm was employed to rank gene importance based on its classification accuracy across decision trees. Genes identified by both methods were considered robust candidates

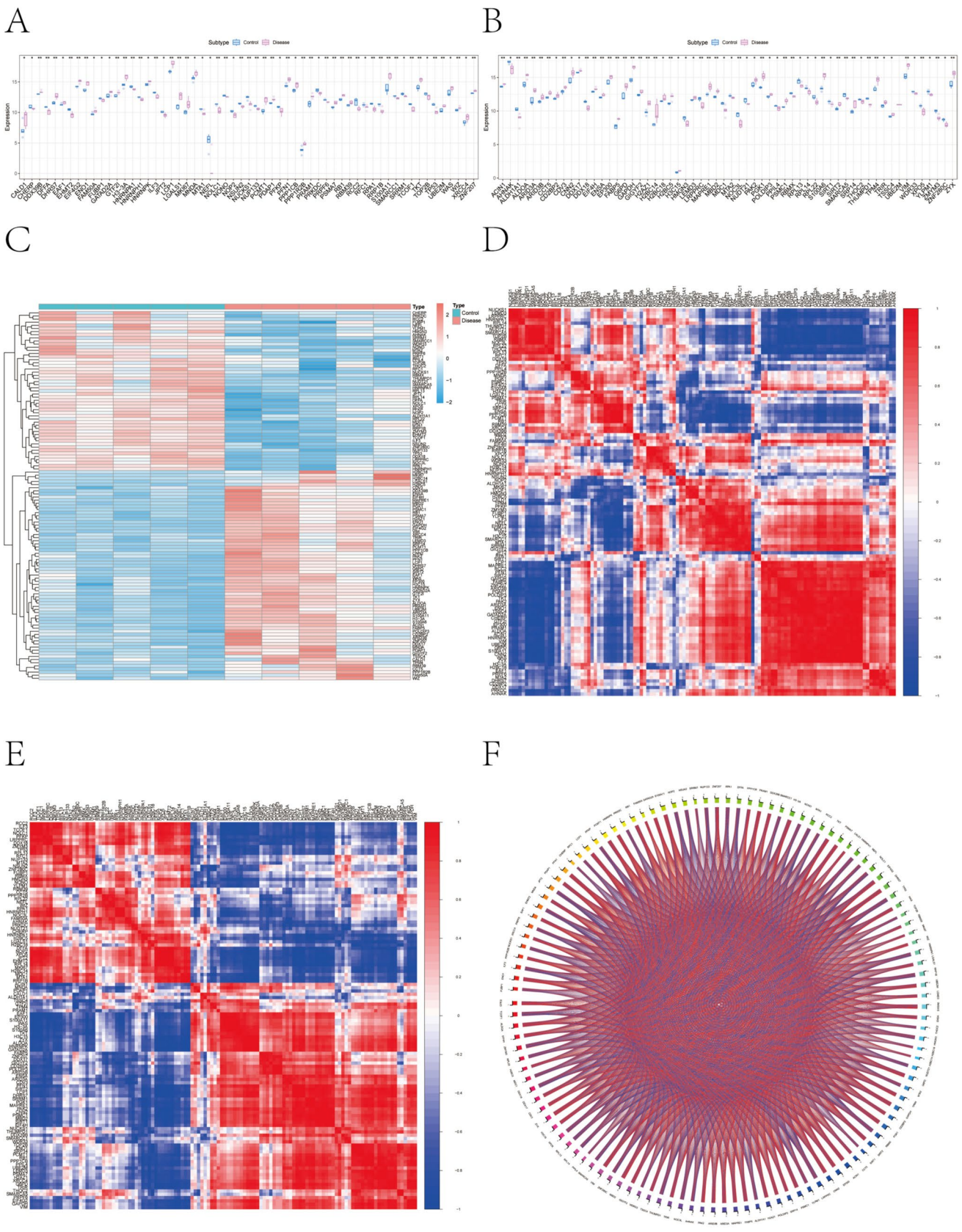
A
B
C
D
E
F
Subtype
Control
Disease
Expression
Type

◂**Fig. 1** Expression Patterns and Co-Expression Analysis of LRGs. **A**, **B** Differential expression of LRGs between two patient groups. Blue represents control samples, while pink represents disease samples. **C** Heatmap of differentially expressed LRGs, where blue indicates low expression and red indicates high expression. **D**, **E** Correlation heatmaps of LRGs, with blue representing negative correlations and red representing positive correlations. **F** Correlation circos plot of LRGs

for further analysis, ensuring consistency across linear and nonlinear models.

Transcriptional regulation analysis of key genes

Transcription factors (TFs) were predicted using the R package RcisTarget. All computations performed by RcisTarget are motif-based. The normalized enrichment score (NES) of a motif depends on the total number of motifs present in the reference database. In addition to motifs annotated in the original data, further annotation files were inferred based on motif similarity and gene sequence information. The first step in estimating the overrepresentation of each motif within a given gene set involves calculating the area under the curve (AUC) for each motif–gene set pair. This is performed by constructing a recovery curve based on the ranking of genes associated with each motif. The NES for each motif is then calculated based on the AUC distribution of all motifs within the gene set.

miRNA network construction

MicroRNAs (miRNAs) are small non-coding RNAs that regulate gene expression by either promoting mRNA degradation or inhibiting mRNA translation. To explore whether miRNAs play a role in regulating the transcription or degradation of critical genes associated with disease, we conducted further analysis. Key gene-related miRNAs were identified using the miRcode database, and the miRNA-gene interaction network was visualized using Cytoscape software.

Single-cell data quality control

The expression profile was initially imported using the Seurat package. Cells were filtered based on the total number of unique molecular identifiers (UMIs) per cell, the number of expressed genes, and the proportion of mitochondrial gene expression. The proportion of mitochondrial gene expression refers to the ratio of mitochondrial gene expression relative to the total gene expression within each cell. A high proportion of mitochondrial gene expression is indicative of cells with reduced RNA expression, suggesting they may be undergoing apoptosis. Quality control was performed using the median absolute deviation (MAD) method. Typically, values that deviate more than 3 MAD from the median are considered outliers and were excluded from the analysis. To further refine the dataset, DoubletFinder (V2.0.4) was used to identify and filter doublets from each sample, completing the cell quality control process.

Dimensionality reduction clustering and cell annotation of single-cell data

We applied the global normalization method, LogNormalize, to adjust the total gene expression of each cell to 10,000 by multiplying by a scaling factor (s0), followed by logarithmic transformation for normalization. Cell cycle scores were calculated using the CellCycleScoring function. Hypervariable genes were identified using the FindVariableFeatures function. To account for gene expression fluctuations associated with mitochondrial gene expression, ribosomal gene expression, and cell cycle effects, we employed the ScaleData function. Linear dimensionality reduction was performed on the expression matrix using principal component analysis (PCA), and principal components were selected for subsequent analysis. To mitigate batch effects, we utilized Harmony for batch correction. Nonlinear dimensionality reduction was achieved using Uniform Manifold Approximation and Projection (UMAP) through the RunUMAP function. For cell-type annotation, we queried the CellMarker and PanglaoDB databases, supplemented by automated annotation using SingleR software, to identify cell types and their corresponding marker genes in the tissue of interest.

Statistical analysis

All statistical analyzes were performed using R language (version 4.2.2), and $p < 0.05$ was considered statistically significant.

Results

Expression patterns and co-expression analysis of LRGs in septic renal injury

In order to explore the expression pattern of LRGs in septic kidney injury, we downloaded the GSE232404 septic kidney injury-related data set from the GEO database and included a total of expression profile data of 10 patients, including the control group (n = 5), disease group (n = 5). Then, 332 LRGs were obtained from the literature [26]. By calculating the expression differences of LRGs between the control group and the disease group, it was found that 118 LRGs had significant differences in expression (Fig. 1A, B), we used these 118 significantly different LRGs as a candidate gene set for subsequent analysis. In addition, we displayed the expression of candidate gene sets in disease and control groups as

a heat map (Fig. 1C), and analyzed the correlation of these candidate gene sets in disease groups and control groups (Fig. 1D, E). And analyze the co-expression of candidate gene sets in sepsis kidney injury data, and use the "corrplot" and "circlize" packages to draw lactation correlation analysis circle diagrams (Fig. 1F).

Pathway enrichment analysis

Subsequently, we performed Gene Set Enrichment Analysis (GSEA) on the candidate gene sets, a widely employed tool for interpreting gene expression data at the gene set, genomic, or regulatory level, particularly for pathways with shared biological functions. Gene Ontology (GO) analysis revealed that the genes were primarily enriched in pathways associated with RNA splicing, regulation of RNA splicing, and histone deacetylation. Kyoto Encyclopedia of Genes and Genomes (KEGG) analysis indicated that the genes were predominantly enriched in pathways related to amino acid biosynthesis, carbon metabolism, and ATP-dependent chromatin remodeling (Fig. 2.A, B).

Immune infiltration analysis

The immune microenvironment consists of immune cells, extracellular matrix components, various growth factors, inflammatory mediators, and distinct physical and chemical characteristics, all of which play a critical role in disease diagnosis and the responsiveness to clinical treatments. We present the distribution of immune infiltration levels and the correlation heatmaps of immune cell types in different formats (Fig. 3A, B). In addition, we observed significant differences in the levels of several immune cell types, including M0 macrophages, neutrophils, resting NK cells, activated CD4 + memory T cells, and resting CD4 + memory T cells, between the disease and control groups (Fig. 3C).

Correlation between LRGs and immune factors

In addition, we examined the correlation between the candidate gene sets and various immune factors, including immunosuppressive factors, immunostimulatory factors, chemokines, and receptors. These analyses revealed that the genes are closely associated with immune cell infiltration levels and play a significant role in modulating the immune microenvironment (Fig. 4A–E). Notably, H3C15 exhibited a significant negative correlation with the immune factor MTA2 (COR = -0.63), whereas PSMC1 showed a significant positive correlation with the immune factor PGK1 (COR = 0.99) (Fig. 4F, G).

Consistent clustering molecular typing and differential expression of immune characteristics across typing

We further employed the consistent clustering method to molecularly classify the disease group based on the expression profiles of the candidate gene sets (Fig. 5A–C). The results indicated that, at K = 2, the sample subtypes were distinctly delineated, thereby dividing septic renal injury

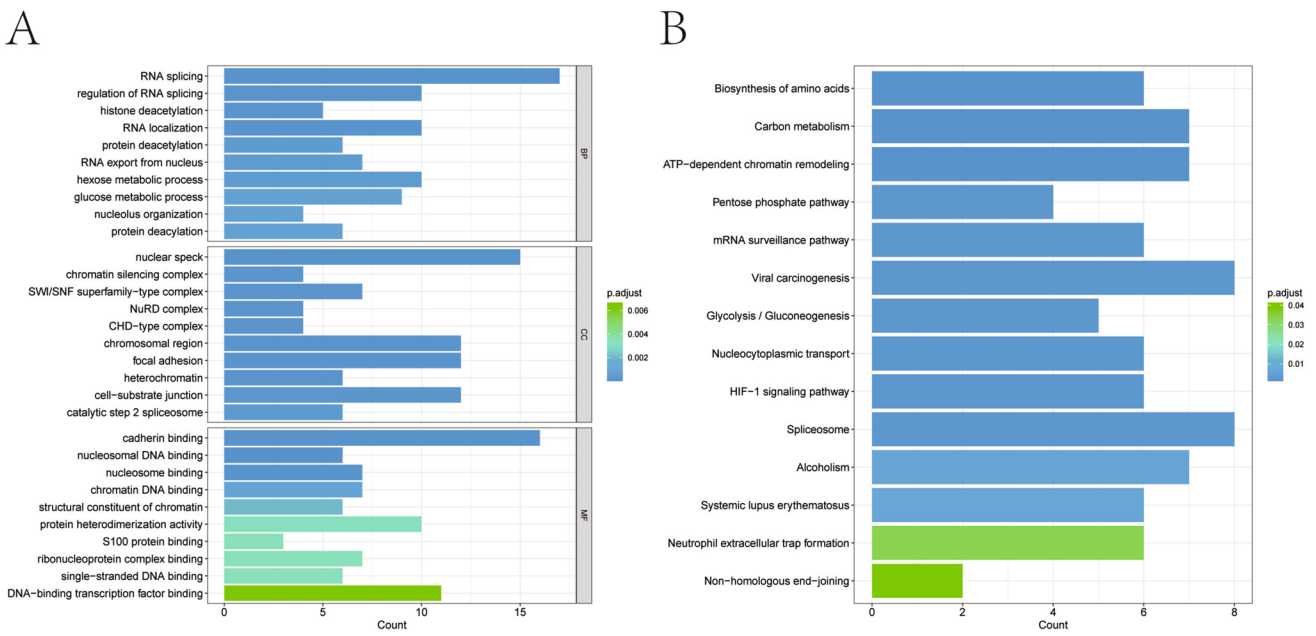

Fig. 2 Enrichment Analysis. **A**, **B** GO and KEGG enrichment analysis based on ClusterProfiler

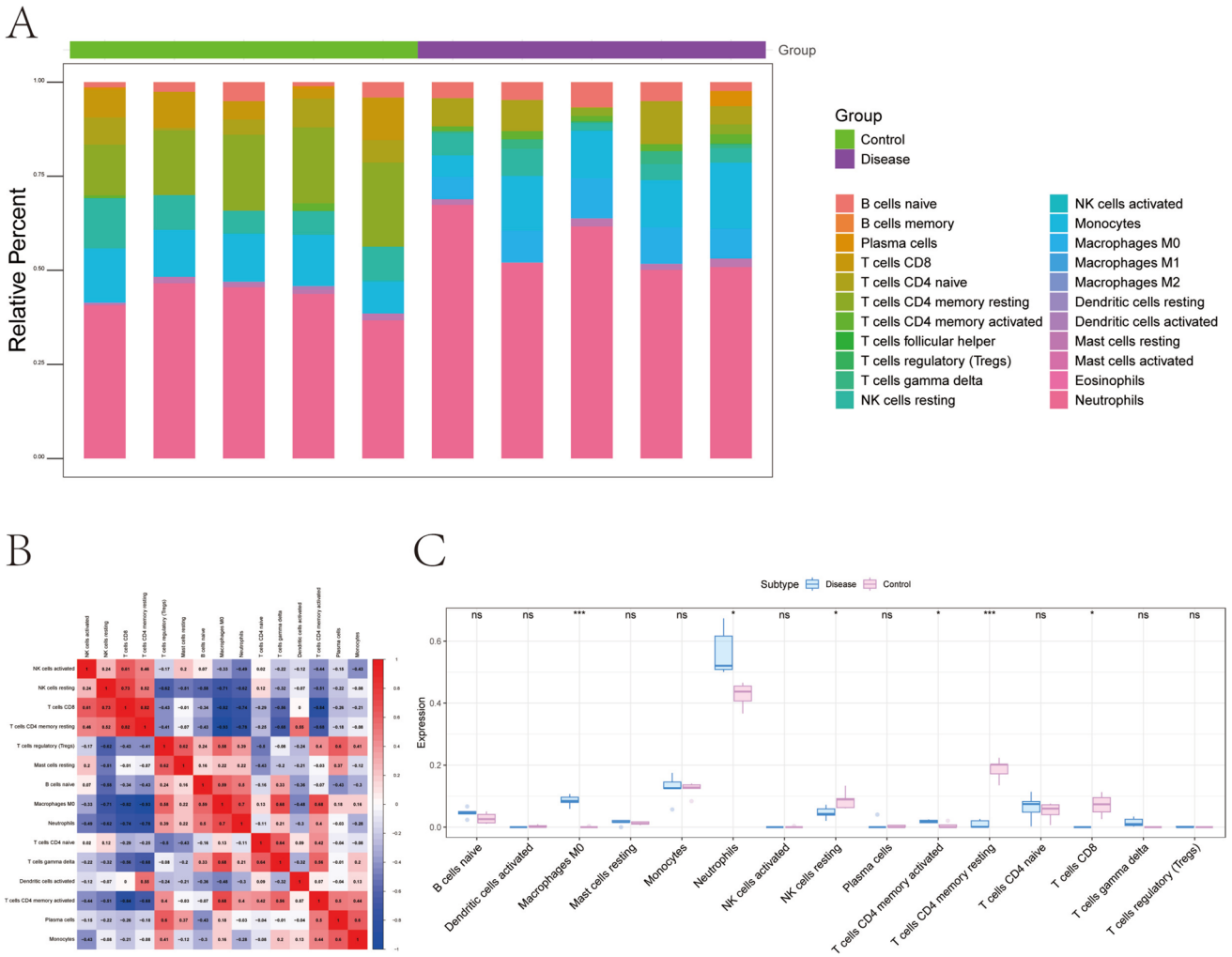

Fig. 3 Immune Infiltration Analysis. **A** Relative proportions of immune cell subpopulations. **B** Correlation between immune cells, with blue indicating negative correlations and red indicating positive correlations. **C** Differences in immune cell composition between control and disease samples

into two distinct clusters. Additionally, we visualized the expression levels of LRGs across the two subtypes using a heatmap (Fig. 5D). In addition, we performed a differential expression analysis to compare immune factors, including immunosuppressive factors, immunostimulatory factors, chemokines, and receptors, between the different subtypes. These analyses revealed significant variations in immune cell infiltration levels across the subtypes (Fig. 6A–E).

Differential expression analysis and functional enrichment analysis across subtypes

To further investigate the expression differences between the subtypes, we utilized the "limma" package to perform differential expression analysis (Fig. 7A,B), identifying genes that were differentially expressed between the subtypes (adj. P.Val < 0.05 and |logFCl> 2), yielding a total of 1,034 subtype-specific differential genes. To better understand the functional roles of these differential genes, we conducted functional enrichment analysis. Gene Ontology (GO) analysis revealed that the subtype-specific differential genes were predominantly enriched in pathways related to T cell differentiation, lymphocyte differentiation, and leukocyte cell–cell adhesion (Fig. 7C). Kyoto Encyclopedia of Genes and Genomes (KEGG) analysis indicated that these genes were mainly enriched in pathways such as cytokine-cytokine-receptor interactions, hematopoietic cell lineage, and viral protein interaction with cytokines and their receptors (Fig. 7D).

WGCNA network analysis associated with subtype classification

To investigate the gene co-expression patterns related to subtype classification, we conducted a weighted gene

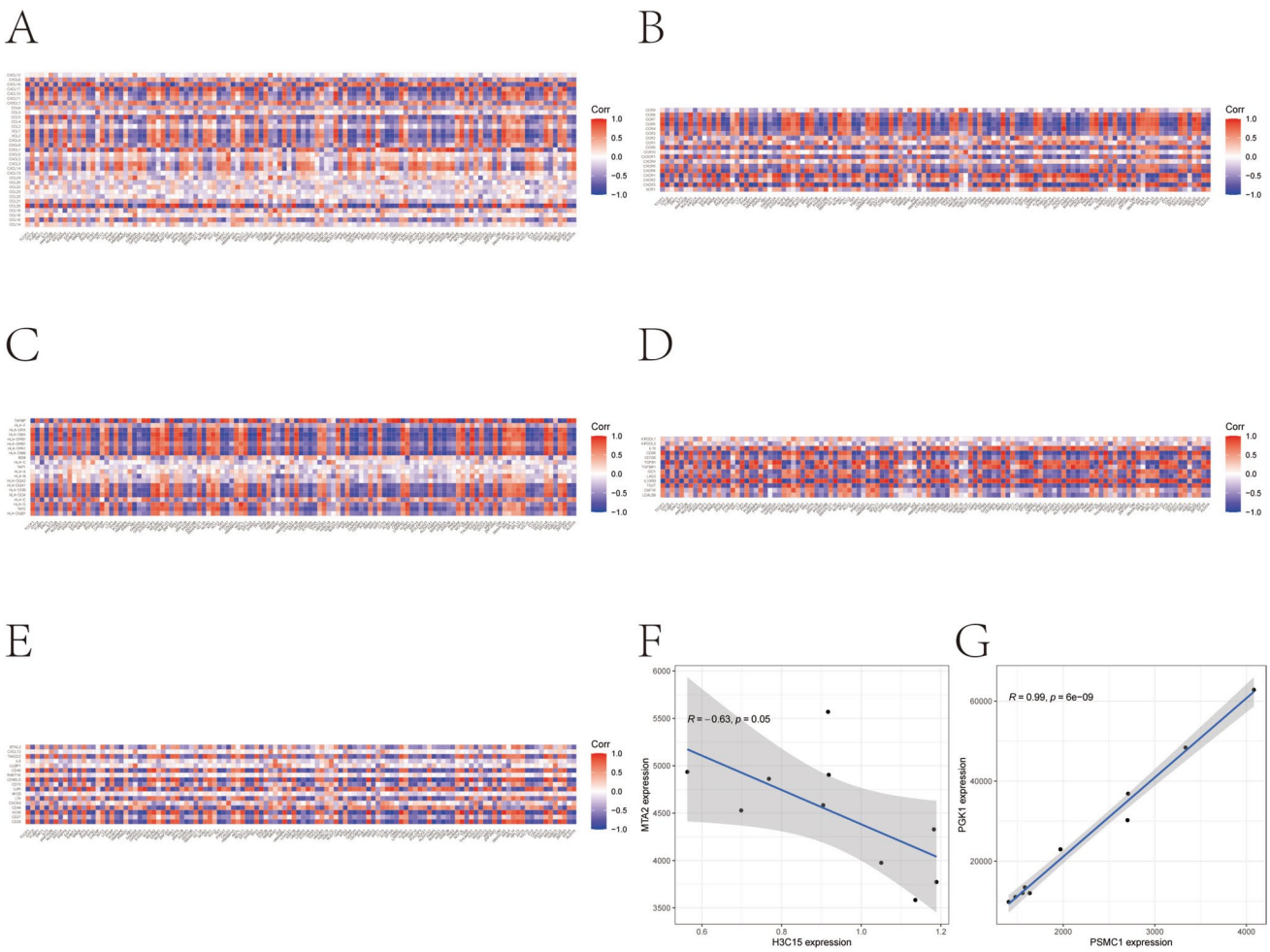

Fig. 4 Correlation Between LRGs and Various Immune Factors. **A**–**E** Correlation analysis between LRGs and immune factors, including chemokines, immunoinhibitors, immunostimulators, MHC molecules, and receptors. **F** Scatter plot of the correlation between H3C15 and the immune factor MTA2. **G** Scatter plot of the correlation between PSMC1 and the immune factor PGK1

co-expression network analysis (WGCNA) based on the expression profiling data. The soft-thresholding power β was determined to be 21 (Fig. 8A, B), and gene modules were subsequently identified using the topological overlap matrix (TOM). This analysis identified a total of seven gene modules (Fig. 8C), among which the darkseagreen3 module exhibited the strongest correlation with subtype classification (cor = 0.96, $p = 1 \times 10^{-5}$). To refine the analysis, we intersected the genes within the darkseagreen3 module with the 1,034 subtype-specific differential genes identified previously, yielding a set of 305 intersecting genes (Fig. 8D).

Machine learning identifies key genes

In order to further pinpoint the key genes influencing septic kidney injury, we utilized the intersecting genes identified in the previous step for feature selection using Lasso regression and random forest algorithms. Lasso regression analysis identified nine characteristic genes associated with septic kidney injury (Fig. 9A, B). Concurrently, the random forest algorithm was employed to screen and rank characteristic genes, yielding the top 10 genes implicated in septic kidney injury (Fig. 9C). Subsequently, we intersected the characteristic genes identified by the Lasso regression and random forest algorithms, resulting in two overlapping genes, PECR and TP53I3 (Fig. 9D). These two genes are proposed as key targets for subsequent investigations into the pathophysiology of septic kidney injury.

Analysis of lactation gene-related transcriptional regulation and construction of miRNA-mRNA network

Key genes were selected as the gene set for transcriptional regulation analysis, revealing their regulation by multiple shared transcription factors. To further investigate these

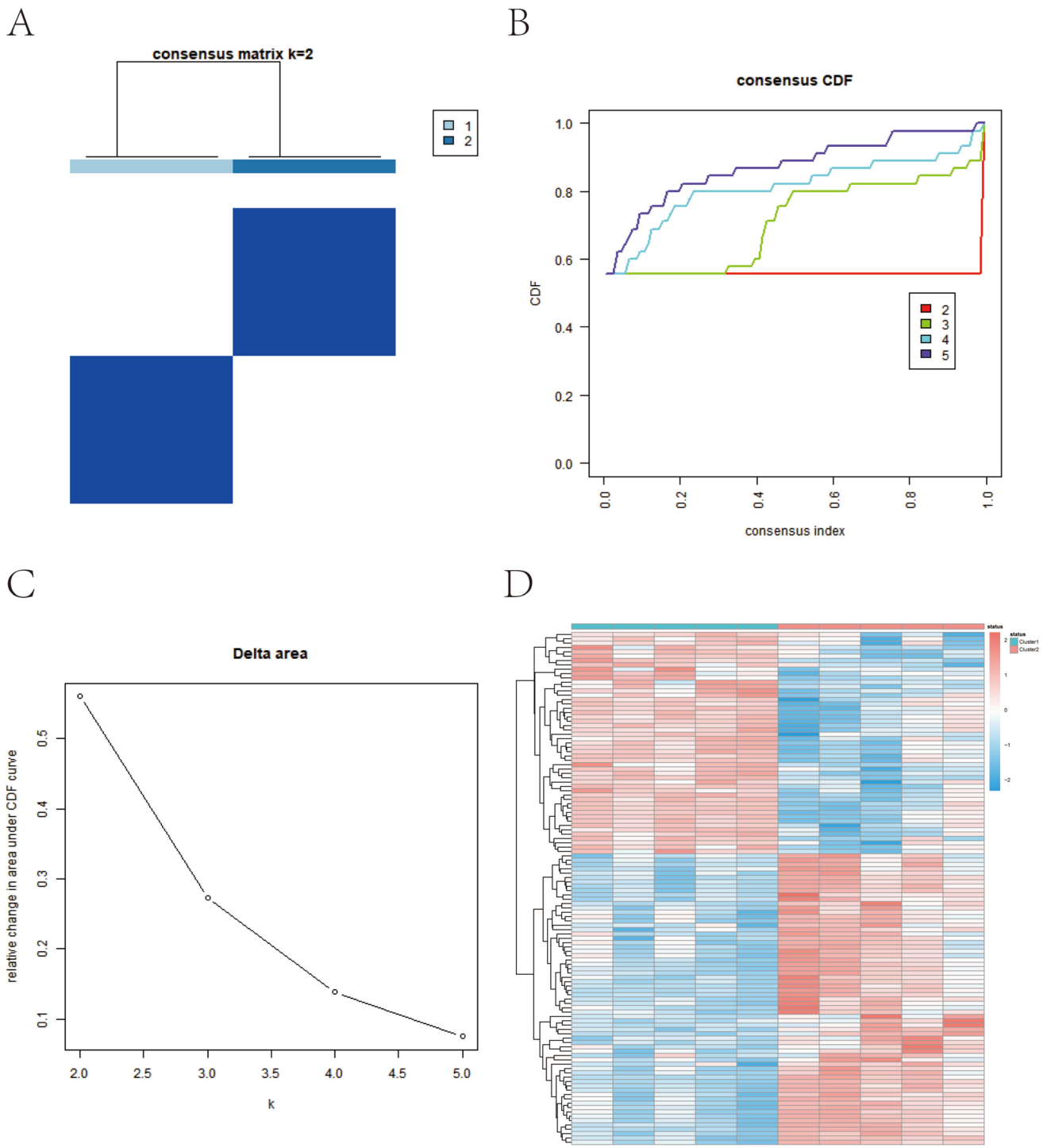

Fig. 5 Subtype Clustering. **A** Consensus clustering of LRGs. **B** CDF curve of LRGs. **C** Delta area plot. **D** Heatmap showing the expression patterns of differentially expressed LRGs across two molecular subtypes of SA-AKI identified via consensus clustering. The color scale represents the standardized Z-score of gene expression, with red indicating higher expression and blue indicating lower expression across samples. Each row represents an individual LRG, and each column corresponds to a SA-AKI sample. Gene expression differences between the clusters were assessed using the Wilcoxon rank-sum test, and genes included in the heatmap met the cutoff criteria of adjusted $p < 0.05$ and |log2 fold change|> 1

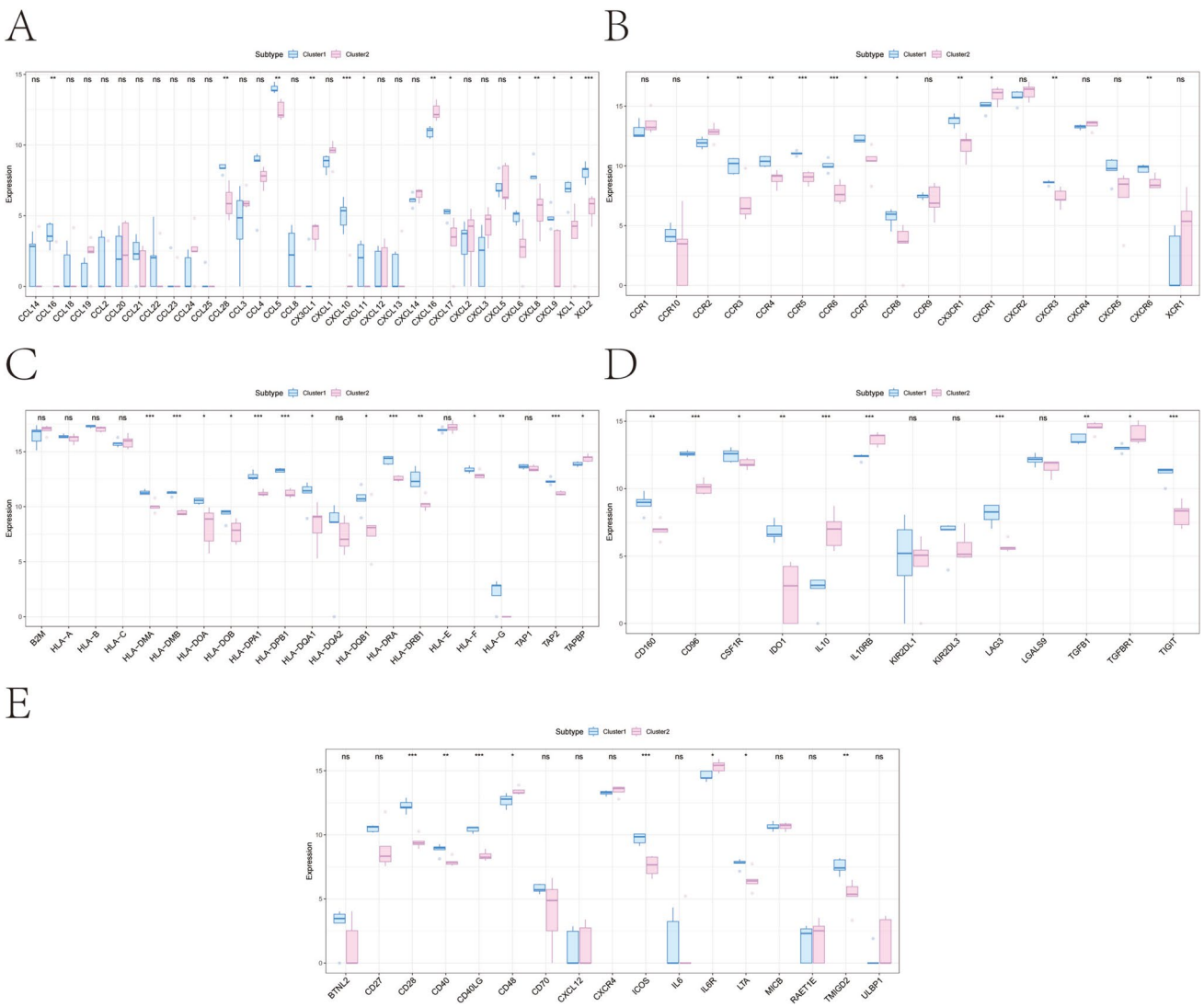

Fig. 6 Differential Expression of Immune Factors Among Subtypes. **A**–**E** Expression differences of chemokines, immunoinhibitors, immunostimulators, MHC molecules, and receptors between SA-AKI molecular subtypes. The y-axis represents normalized gene expression levels, and the x-axis lists individual immune checkpoint genes. Each box shows the interquartile range (IQR), with the median indicated by a horizontal line, while the violin shape reflects the distribution density. Group comparisons were performed using the Wilcoxon rank-sum test. Statistical significance is denoted as follows: * $p<0.05$, ** $p<0.01$,*** $p<0.001$,"ns" indicates no statistically significant difference ($p\geq0.05$)

regulatory mechanisms, we performed enrichment analysis of transcription factors using cumulative recovery curves and motif-TF annotation. Among the identified motifs, cisbp__M1413 exhibited the highest normalized enrichment score (NSE = 14). A comprehensive visualization of all enriched motifs and their corresponding transcription factors regulating LRGs is provided (Fig. 10B). Additionally, reverse prediction of the two key genes was conducted using the miRcode database, identifying 40 miRNAs and uncovering a total of 47 mRNA-miRNA regulatory pairs. These interactions were visualized using Cytoscape to construct a miRNA-mRNA regulatory network, providing insights into the post-transcriptional regulatory landscape of the key genes (Fig. 10A-C).

Single-cell quality control and data standardization

To ensure high data quality across multiple samples, cells with fewer than 200 detected genes were excluded from further analysis. The filtering criteria applied were as follows: (nFeature_RNA > 200 & percent.mt < = median + 3MAD & nFeature_RNA < = median + 3MAD & nCount_RNA < = median + 3MAD), where nFeature_RNA represents the number of genes, nCount_RNA represents the

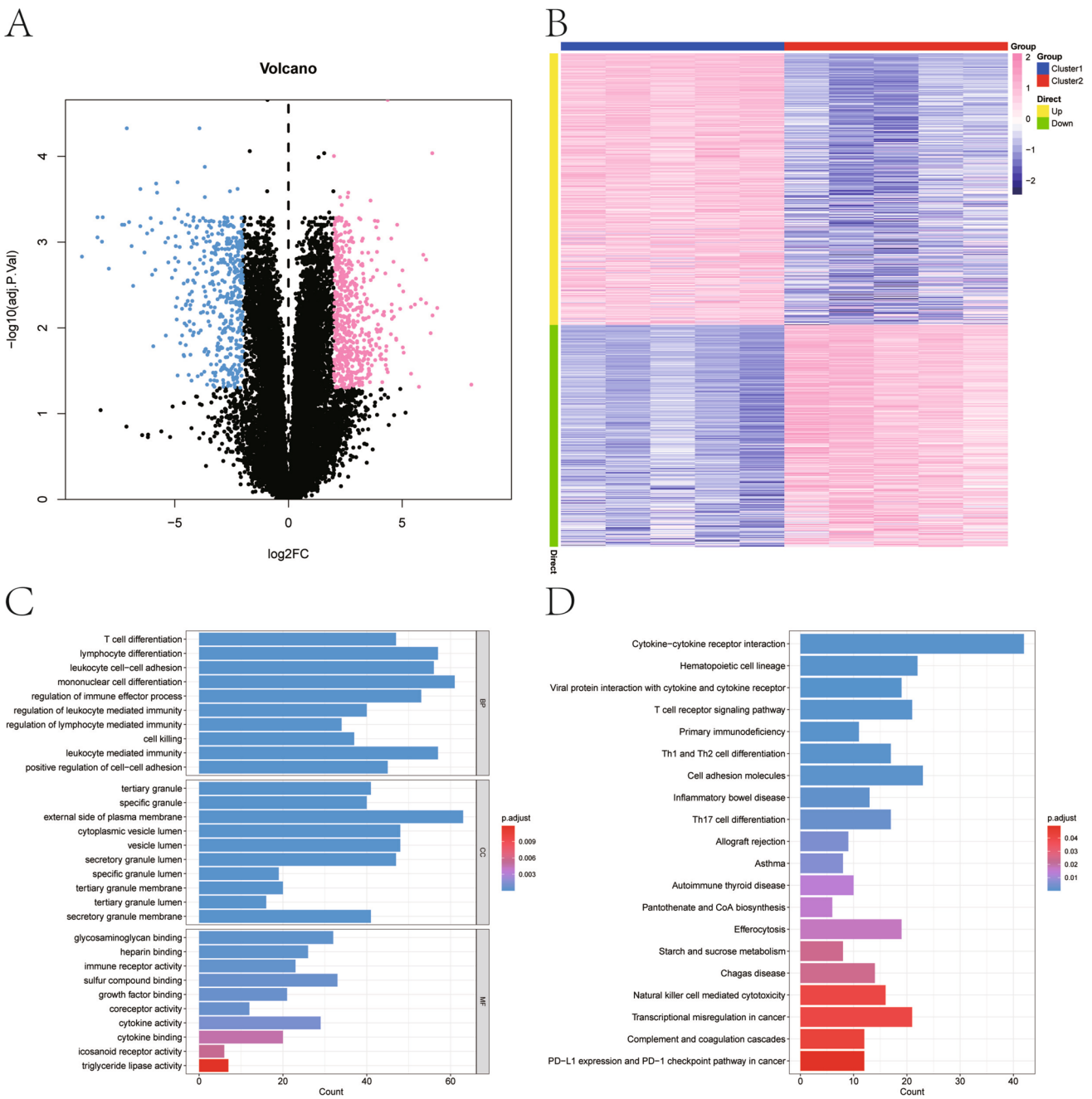

Fig. 7 Differential and Enrichment Analysis of Subtypes. **A** Volcano plot of differentially expressed genes (DEGs) between subtypes, with blue indicating downregulated genes and pink indicating upregulated genes. **B** Heatmap of differentially expressed genes among subtypes, where blue represents low expression and pink represents high expression. **C**, **D** GO and KEGG enrichment analysis based on ClusterProfiler

total number of UMIs of the cell, and percent.mt represents the percentage of mitochondrial reads. To further eliminate potential doublets, the DoubletFinder package was employed, resulting in the retention of 16,323 high-quality cells. Quality control results, including violin and scatter plots, are presented in Supplemental Fig. 2A-B. Subsequently, 2,000 highly variable genes were identified for downstream analysis (Supplemental Fig. 2C). Standardization and normalization were performed, followed by principal component analysis (PCA) and batch correction using harmony analysis to mitigate batch effects and ensure data consistency (Supplemental Fig. 2D-F).

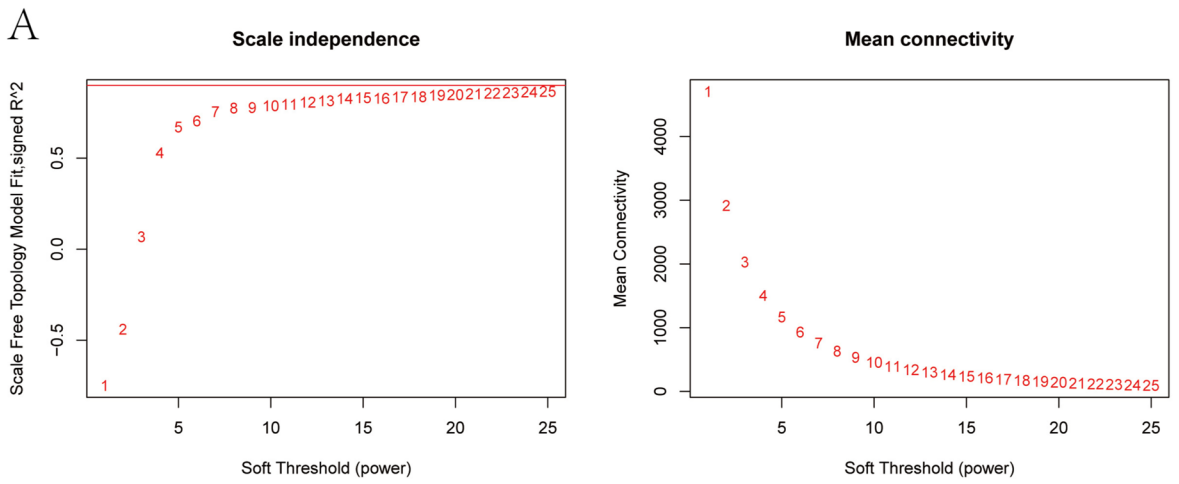
A
Scale independence
Scale Free Topology Model Fit,signed R^2
Soft Threshold (power)
Mean connectivity
Mean Connectivity
Soft Threshold (power)

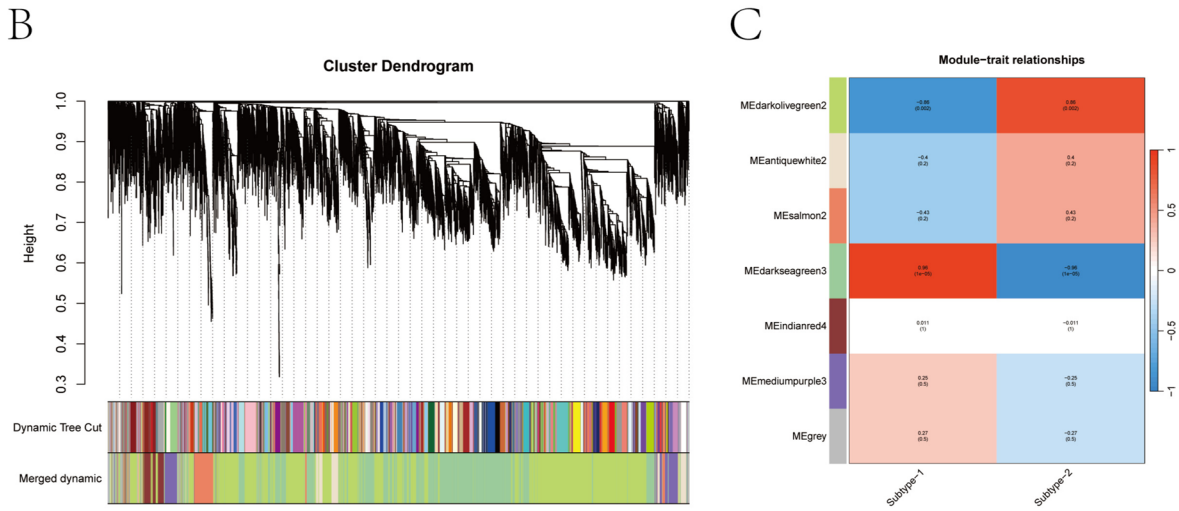
B
Cluster Dendrogram
Height
Dynamic Tree Cut
Merged dynamic
C
Module−trait relationships
MEdarkolivegreen2
MEantiquewhite2
MEsalmon2
MEdarkseagreen3
MEindianred4
MEmediumpurple3
MEgrey
Subtype−1
Subtype−2

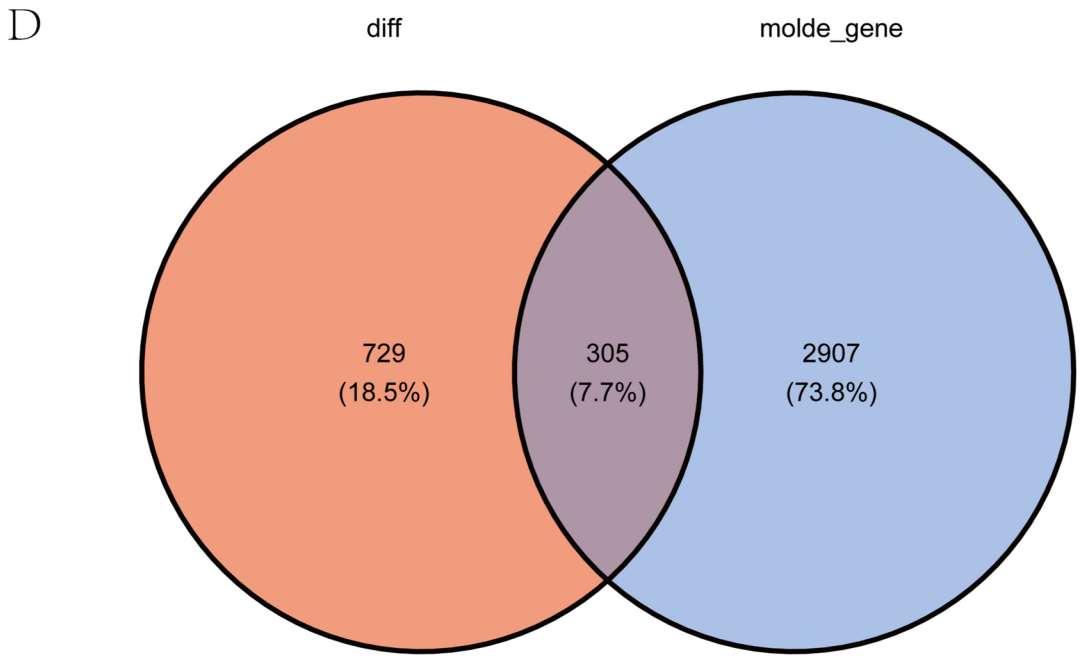
D
diff
molde_gene
729
(18.5%)
305
(7.7%)
2907
(73.8%)

◂**Fig. 8** WGCNA Analysis of Subtypes. **A** Scale-free index and average connectivity for each soft threshold. **B** Gene clustering dendrogram, with different colors representing distinct modules. **C** Correlation between module characteristic genes and subtypes, with blue indicating negative correlations and red indicating positive correlations. **D** Venn diagram showing the intersection of differential genes and key module genes

Cell Annotation and expression abundance of key genes

Using UMAP for dimensionality reduction, nine distinct cell subgroups were identified (Fig. 11A). Further annotation of these subgroups classified them into seven major cell types: proximal tubule cells, epithelial cells, loop of Henle cells, intercalated cells, endothelial cells, monocytes, and mesangial cells (Fig. 11B). A bubble chart depicting the classic markers for these seven cell types (Fig. 11C) and a histogram illustrating the cell-type proportions across different groups (Fig. 11D) were generated to provide a comprehensive overview of cell classification. To investigate the expression patterns of key genes, we utilized the DotPlot and FeaturePlot functions in the Seurat R package to visualize their distribution across single-cell data (Fig. 11E,F). Additionally, LRGs expressed in the single-cell dataset were selected to explore their co-expression networks with key genes via correlation analysis. Notably, TP53I3 showed a significant positive correlation with HDAC2 (COR = 0.58) (Supplemental Fig. 3A-C), while PECR and HDAC3 exhibited a significant negative correlation (COR = -0.79) (Supplemental Fig. 4A-C).

Discussion

Acute kidney injury (AKI) is a common and severe clinical syndrome with high incidence and mortality rates, representing a significant global public health challenge. Epidemiological data indicate that more than 40% of sepsis patients develop AKI, a complication that markedly increases hospitalization duration, treatment costs, and the risk of long-term adverse outcomes[27, 28]. Despite advancements in the diagnosis and treatment of sepsis-associated AKI (SA-AKI), the complex pathophysiological mechanisms and substantial inter-individual heterogeneity present significant challenges for precise management[29, 30]. Consequently, exploring the molecular mechanisms of SA-AKI and identifying key regulatory genes are crucial for optimizing diagnosis and promoting individualized treatment.

The rapid development of molecular biology and genomics has created new opportunities for the early diagnosis and targeted therapy of SA-AKI. By analyzing key genes and their regulatory networks, it is possible to elucidate the mechanisms underlying SA-AKI and provide a theoretical basis for precision medical interventions[19, 31]. In this study, the pathway enrichment analysis revealed significant involvement of RNA splicing, histone deacetylation, and carbon metabolism in SA-AKI. These biological processes may contribute to the pathophysiological mechanisms underlying sepsis-induced kidney injury. Aberrant RNA splicing has been implicated in modulating inflammatory responses and apoptosis, two hallmark features of SA-AKI. Non-coding RNAs such as miRNAs and lncRNAs can regulate splicing machinery and influence the expression of genes related to cell death and immune activation[32]. Histone deacetylation, particularly via SIRT1, has been shown to exert protective effects in SA-AKI by deacetylating HMGB1 and suppressing its pro-inflammatory activity. This epigenetic regulation attenuates renal inflammation and cellular damage[33]. Furthermore, carbon metabolism undergoes a profound shift during SA-AKI. Renal tubular epithelial cells switch from oxidative phosphorylation to glycolysis, resulting in increased lactate accumulation[34]. Elevated lactate levels can promote protein lactylation, a newly recognized post-translational modification that may modulate gene expression involved in immune responses and metabolic stress. These findings collectively suggest that the enriched pathways are not only involved in SA-AKI pathogenesis but may also intersect with lactylation-related regulatory networks, warranting further investigation.

Lactylation, as an emerging form of epigenetic modification, is closely associated with metabolic reprogramming and inflammatory responses, both of which play pivotal roles in the pathogenesis of SA-AKI[35–37]. By performing differential analysis of bulk expression profiles, we identified 118 lactylation-related differentially expressed genes (DEGs) and used consensus clustering to stratify patient samples. The results revealed two distinct subtypes with significant differences in lactylation gene expression and immune microenvironment characteristics. Subtype 1 exhibited higher levels of immune infiltration, while Subtype 2 showed relatively lower immune activity, suggesting that lactylation modifications may influence disease progression by modulating differential patterns of immune cell infiltration. Enrichment analysis further indicated that DEGs between the two subtypes were predominantly enriched in immune- and inflammation-related pathways, such as cytokine-receptor interactions and T cell differentiation pathways. The activation of these pathways is closely associated with the inflammatory response in SA-AKI and plays a critical role in disease progression.

Immune infiltration plays a key role in the onset and progression of SA-AKI and has become a hot topic in recent research. The inflammatory response triggered by sepsis can lead to excessive activation and dysregulation of the immune system, resulting in kidney tissue damage[29, 38]. The CIBERSORT-based immune infiltration analysis revealed a significant increase in M0 macrophages, neutrophils, and activated CD4 memory T cells in SA-AKI kidney tissue,

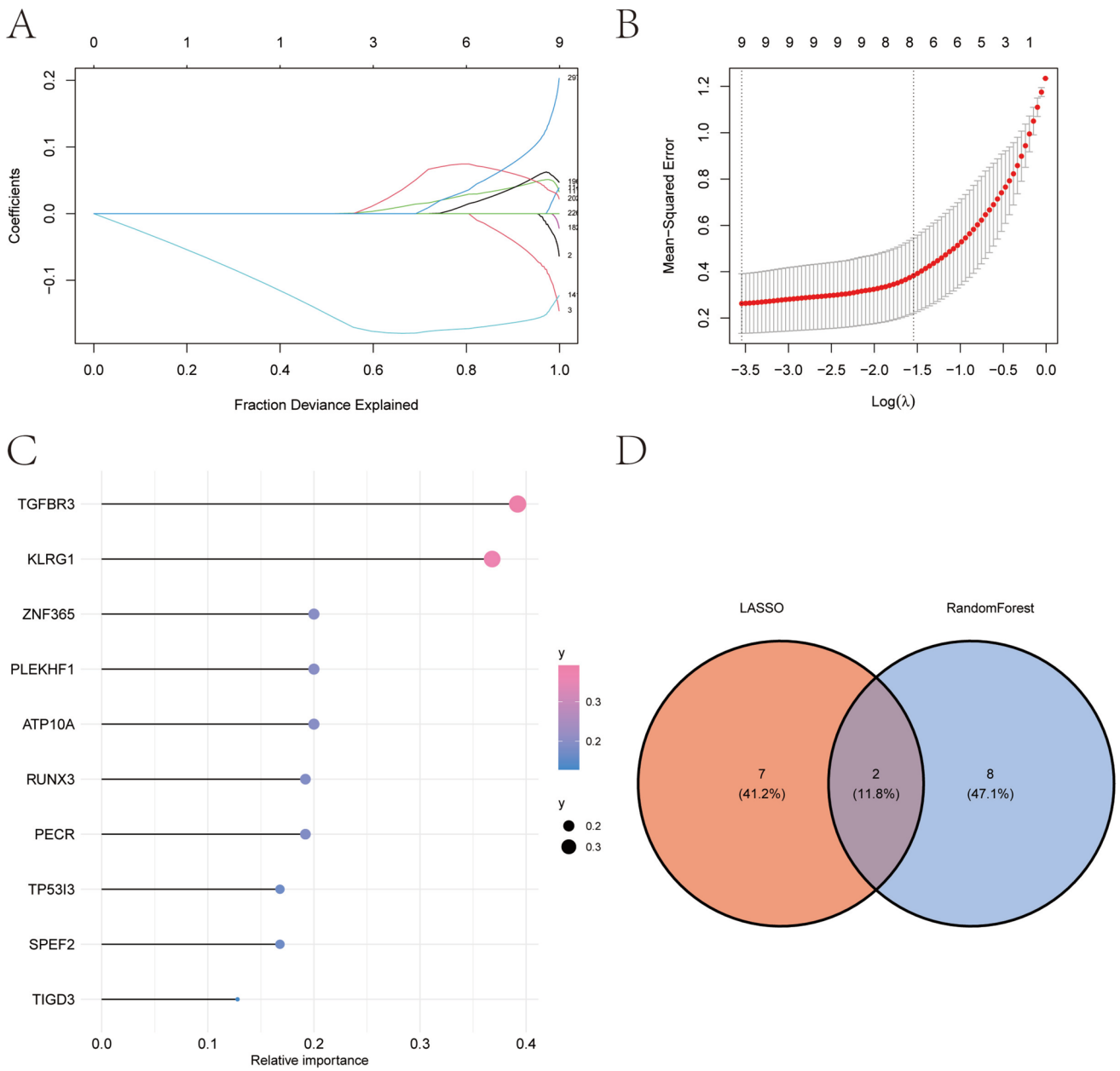

Fig. 9 Construction of Lasso and Random Forest Models. **A** Distribution of LASSO coefficients and gene combinations at the minimum lambda value. **B** Ten-fold cross-validation for the selection of tuning parameters in the LASSO model to determine the minimum lambda value. **C** Visualization of feature genes selected by the random forest model. **D** Intersection of feature genes identified by Lasso regression and random forest models

highlighting an immunologically active microenvironment. M0 macrophages, as unpolarized precursors, are pivotal regulators of immune responses. Their expansion in SA-AKI may reflect either a delayed or dysfunctional polarization toward M1/M2 phenotypes. This dysregulation could impair the resolution of inflammation and contribute to prolonged tissue injury. Studies have shown that in sepsis, the balance between M1 (pro-inflammatory) and M2 (pro-repair) macrophages is often disrupted, potentially leading to persistent renal damage and maladaptive repair [39]. Neutrophils are among the first responders in sepsis and are known to aggravate acute kidney injury through degranulation, release of ROS, and formation of neutrophil extracellular traps (NETs), which can damage endothelial and epithelial barriers [40]. Activated CD4 memory T cells may contribute to immune dysregulation by producing pro-inflammatory cytokines and perpetuating renal inflammation. Their presence in SA-AKI suggests the involvement of adaptive immune memory in

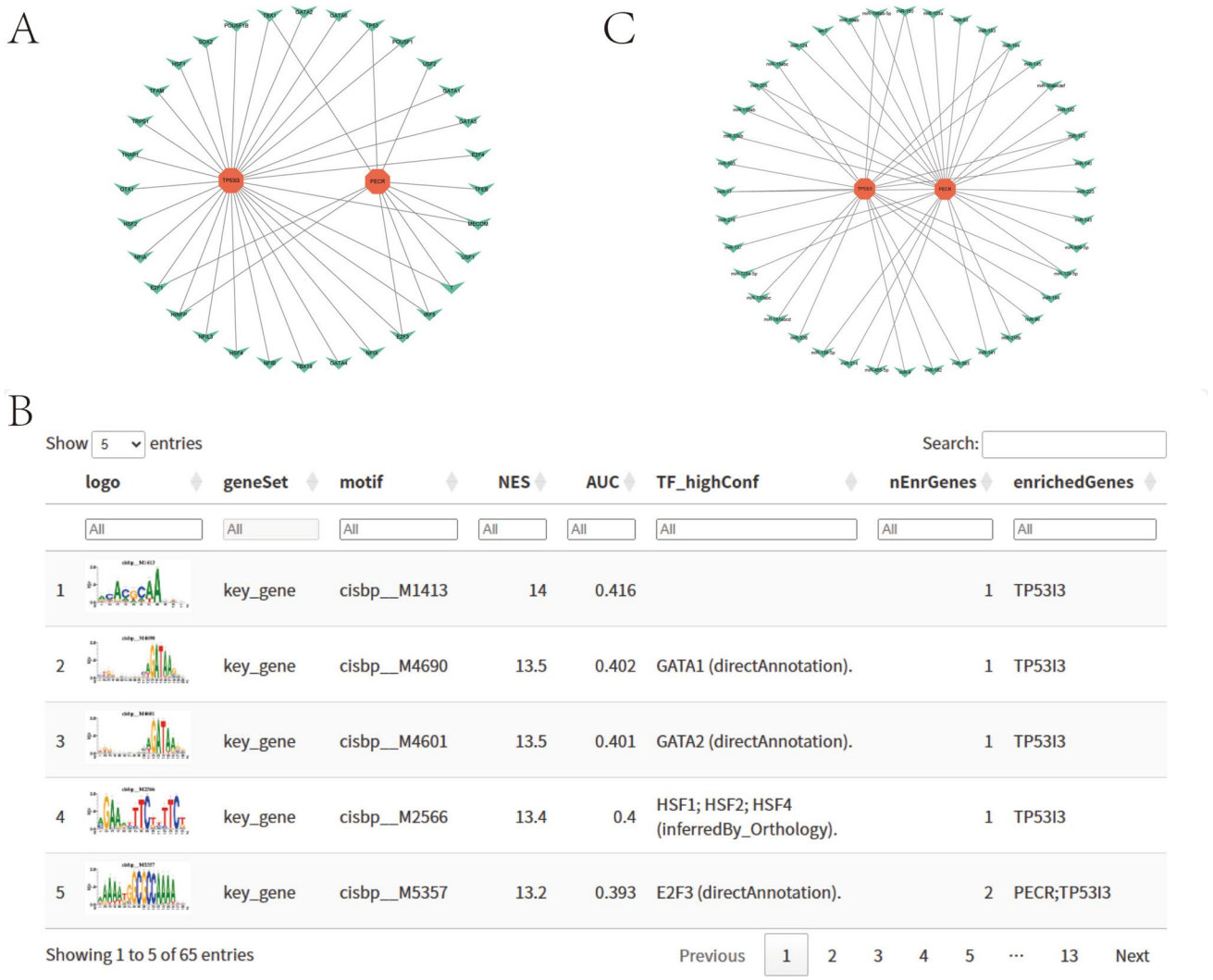

Fig. 10 Transcriptional Regulation and miRNA Network of Key Genes. **A** Transcriptional regulation network of key genes, with red representing key genes and gray representing transcription factors. **B** Motifs enriched by key genes and their corresponding transcription factors are displayed. **C** miRNA network of key genes, with red representing mRNA and gray representing miRNA

sustaining injury, even after the initial septic insult. Collectively, these immune alterations suggest not merely bystander activation, but a coordinated dysregulation of innate and adaptive immune responses actively shaping the course of SA-AKI. In this study, immune cell characteristic analysis revealed significant upregulation of Macrophages M0, Neutrophils, and T cells CD4 memory activated in the disease group. In addition, the expression of LRGs was significantly correlated with immune factors, such as a negative correlation between H3C15 and the immune-suppressive factor MTA2, and a positive correlation between PSMC1 and the immune-stimulatory factor PGK1. These findings suggest that lactylation modifications may influence the immune microenvironment by regulating the expression of immune factors, thereby mediating the pathological processes of kidney injury.

The identification of PECR and TP53I3 as key genes through consensus clustering and machine learning techniques further elucidates the molecular regulatory mechanisms of SA-AKI. PECR plays a critical role in lipid metabolism, particularly in peroxisomal β-oxidation. Its expression is involved in regulating fatty acid metabolism, which can modulate inflammatory processes. Recent studies suggest that PECR expression is altered in various inflammatory diseases, highlighting its potential role in regulating immune responses and contributing to tissue damage in conditions such as sepsis and acute kidney injury. Increased expression of PECR has been linked to oxidative stress and inflammation, which are key mechanisms in SA-AKI pathogenesis. TP53I3 is a p53-inducible gene that is involved in regulating apoptosis and cellular stress responses. It is known to be upregulated under conditions of DNA damage and oxidative

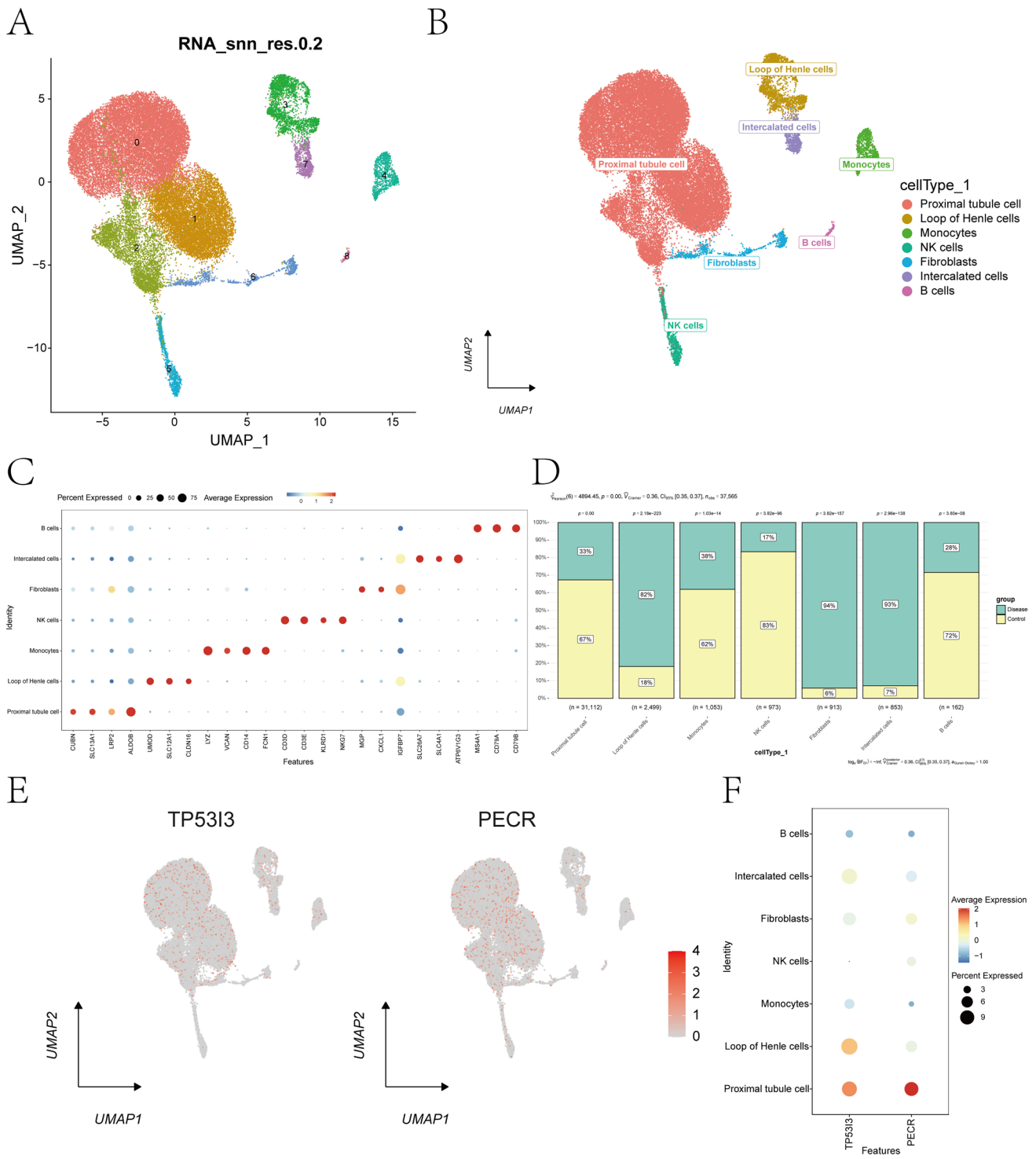

Fig. 11 Cell annotation and expression of key genes in single cells. **A** Cell clustering using the UMAP algorithm, based on important components from PCA, dividing cells into 9 clusters. **B** Cell annotations of the 9 clusters, where the 9 clusters are annotated into 7 cell types: Proximal tubule cells, Epithelial cells, Loop of Henle cells, Intercalated cells, Endothelial cells, Monocytes, and Mesangial cells. **C** Dot-plot bubble plot showing the 7 cell types and their corresponding cell markers. **D** Differences in the proportion of each of the 7 cell types between the two sample groups. **E** Scatter plot of key gene expression profiles in single cells. **F** Bubble plot of key gene expression profiles in single cells, where blue indicates low expression and red indicates high expression

stress, and its role in inflammation is becoming increasingly recognized. TP53I3 has been shown to influence cell survival in response to injury, suggesting its involvement in inflammatory pathways. Evidence from various studies indicates that TP53I3 expression may be upregulated in inflammatory diseases, supporting its potential as a therapeutic target in conditions like SA-AKI.

In conclusion, this study highlights the crucial role of LRGs in SA-AKI and, through molecular subtyping, key gene identification, and immune infiltration analysis, provides valuable insights into the molecular mechanisms and personalized diagnosis and treatment of SA-AKI. PECR and TP53I3, as potential lactylation targets, may offer new therapeutic avenues to improve clinical outcomes for SA-AKI. However, several limitations of this study should be acknowledged. First, the transcriptomic analysis and molecular subtyping were based on a single publicly available dataset, which may limit the generalizability and robustness of the findings. Although internal validation analyses, such as chi-square tests and ROC curve assessments, were performed to support the reliability of the consensus clustering, external validation using independent cohorts is still warranted. Second, due to the limited metadata provided in the original dataset, critical clinical information—such as AKI staging, treatment response, and long-term outcomes—was unavailable. As a result, we were unable to assess the correlation between molecular subtypes and clinical characteristics. Future studies incorporating larger sample sizes and detailed clinical annotations are needed to validate and extend our findings. The regulatory mechanisms of target genes in sepsis-associated kidney injury need to be further validated through basic experiments.

Supplementary Information The online version contains supplementary material available at https://doi.org/10.1007/s10238-025-01745-5.

Acknowledgements We thank all contributors to the GEO database and all developers of the analysis methods and tools mentioned in the article.

Author contributions HX Y, K J, Y C and LY Z conceived the study. K J, SJ M and J L analyzed the data. K J, HX Y, LY Z and HX Z participated in the writing and submission of the manuscript. All authors contributed to the article and approved the submitted version.

Funding No external funding was used.

Data availability The datasets presented in this study can be found in online repositories. The names of the repositories/repositories and accession number(s) can be found in the article/supplementary material.

Declarations

Conflict of interest The authors declare that the research was conducted in the absence of any commercial or financial relationships that could be construed as a potential conflict of interest.

Ethical approval All datasets in this study were downloaded from the public database GEO. These public databases allow researchers to download and analyze datasets for scientific purposes; thus, ethical approval is not required.

Consent for publication All authors have made a substantial contribution to this article and consent to publication.

Open Access This article is licensed under a Creative Commons Attribution-NonCommercial-NoDerivatives 4.0 International License, which permits any non-commercial use, sharing, distribution and reproduction in any medium or format, as long as you give appropriate credit to the original author(s) and the source, provide a link to the Creative Commons licence, and indicate if you modified the licensed material. You do not have permission under this licence to share adapted material derived from this article or parts of it. The images or other third party material in this article are included in the article's Creative Commons licence, unless indicated otherwise in a credit line to the material. If material is not included in the article's Creative Commons licence and your intended use is not permitted by statutory regulation or exceeds the permitted use, you will need to obtain permission directly from the copyright holder. To view a copy of this licence, visit http://creativecommons.org/licenses/by-nc-nd/4.0/.

References

1. Peerapornratana S, Manrique-Caballero CL, Gómez H, Kellum JA. Acute kidney injury from sepsis: current concepts, epidemiology, pathophysiology, prevention and treatment. Kidney Int. 2019;96(5):1083–99.
2. Kellum JA, Prowle JR. Paradigms of acute kidney injury in the intensive care setting. Nat Rev Nephrol. 2018;14(4):217–30.
3. Poston JT, Koyner JL. Sepsis associated acute kidney injury. BMJ. 2019;364:k4891.
4. Dellinger RP, Levy MM, Rhodes A, Annane D, Gerlach H, Opal SM, Sevransky JE, Sprung CL, Douglas IS, Jaeschke R, et al. Surviving Sepsis Campaign: international guidelines for management of severe sepsis and septic shock, 2012. Intensive Care Med. 2013;39(2):165–228.
5. Zhitkovich A. N-acetylcysteine: antioxidant, aldehyde scavenger, and more. Chem Res Toxicol. 2019;32(7):1318–9.
6. Strzelec M, Detka J, Mieszczak P, Sobocińska MK, Majka M. Immunomodulation-a general review of the current state-of-the-art and new therapeutic strategies for targeting the immune system. Front Immunol. 2023;14:1127704.
7. Kounatidis D, Vallianou NG, Psallida S, Panagopoulos F, Margellou E, Tsilingiris D, Karampela I, Stratigou T, Dalamaga M. Sepsis-associated acute kidney injury: Where are we now? Medicina (Kaunas) 2024;60(3).
8. Kellum JA, Lameire N. Diagnosis, evaluation, and management of acute kidney injury: a KDIGO summary (Part 1). Crit Care. 2013;17(1):204.
9. Aguilar MG, AlHussen HA, Gandhi PD, Kaur P, Pothacamuri MA, Talikoti MAH, Avula N, Shekhawat P, Silva AB, Kaur A, et al. Sepsis-associated acute kidney injury: pathophysiology and treatment modalities. Cureus. 2024;16(12):e75992.
10. Fiorentino M, Philippe R, Palumbo CA, Prenna S, Cantaluppi V, Rosa S. Epigenetic mechanisms in sepsis-associated acute kidney injury. Semin Respir Crit Care Med. 2024;45(4):491–502.
11. Mantzarlis K, Tsolaki V, Zakynthinos E. Role of oxidative stress and mitochondrial dysfunction in sepsis and potential therapies. Oxid Med Cell Longev. 2017;2017:5985209.

12. Schulte W, Bernhagen J, Bucala R. Cytokines in sepsis: potent immunoregulators and potential therapeutic targets–an updated view. Mediat Inflamm. 2013;2013:165974.
13. Zhang YY, Ning BT. Signaling pathways and intervention therapies in sepsis. Signal Transduct Target Ther. 2021;6(1):407.
14. Shi J, Zhao Y, Wang K, Shi X, Wang Y, Huang H, Zhuang Y, Cai T, Wang F, Shao F. Cleavage of GSDMD by inflammatory caspases determines pyroptotic cell death. Nature. 2015;526(7575):660–5.
15. Ye Z, Zhang L, Li R, Dong W, Liu S, Li Z, Liang H, Wang L, Shi W, Malik AB, et al. Caspase-11 mediates pyroptosis of tubular epithelial cells and septic acute kidney injury. Kidney Blood Press Res. 2019;44(4):465–78.
16. Bagshaw SM, Uchino S, Bellomo R, Morimatsu H, Morgera S, Schetz M, Tan I, Bouman C, Macedo E, Gibney N, et al. Septic acute kidney injury in critically ill patients: clinical characteristics and outcomes. Clin J Am Soc Nephrol. 2007;2(3):431–9.
17. Murugan R, Kellum JA. Acute kidney injury: What's the prognosis? Nat Rev Nephrol. 2011;7(4):209–17.
18. Qin S, Bai Y, Liu H. Methods and applications of single-cell proteomics analysis based on mass spectrometry. Se Pu. 2021;39(2):142–51.
19. Qiao J, Cui L. Multi-omics techniques make it possible to analyze sepsis-associated acute kidney injury comprehensively. Front Immunol. 2022;13:905601.
20. Tang Y, Yang X, Shu H, Yu Y, Pan S, Xu J, Shang Y. Bioinformatic analysis identifies potential biomarkers and therapeutic targets of septic-shock-associated acute kidney injury. Hereditas. 2021;158(1):13.
21. Akbari B, Huber BR, Sherman JH. Unlocking the hidden depths: multi-modal integration of imaging mass spectrometry-based and molecular imaging techniques. Crit Rev Anal Chem. 2025;55(1):109–38.
22. Mohr AE, Ortega-Santos CP, Whisner CM, Klein-Seetharaman J, Jasbi P. Navigating challenges and opportunities in multi-omics integration for personalized healthcare. Biomedicines 2024;12(7).
23. Zhang D, Tang Z, Huang H, Zhou G, Cui C, Weng Y, Liu W, Kim S, Lee S, Perez-Neut M, et al. Metabolic regulation of gene expression by histone lactylation. Nature. 2019;574(7779):575–80.
24. Deng X, Huang Y, Zhang J, Chen Y, Jiang F, Zhang Z, Li T, Hou L, Tan W, Li F. Histone lactylation regulates PRKN-Mediated mitophagy to promote M2 Macrophage polarization in bladder cancer. Int Immunopharmacol. 2025;148:114119.
25. Shu M, Lu D, Zhu Z, Yang F, Ma Z. Insight into the roles of lactylation in macrophages: functions and clinical implications. Clin Sci (Lond) 2025;139(2).
26. Huang H, Chen K, Zhu Y, Hu Z, Wang Y, Chen J, Li Y, Li D, Wei P. A multi-dimensional approach to unravel the intricacies of lactylation related signature for prognostic and therapeutic insight in colorectal cancer. J Transl Med. 2024;22(1):211.
27. Zarbock A, Nadim MK, Pickkers P, Gomez H, Bell S, Joannidis M, Kashani K, Koyner JL, Pannu N, Meersch M, et al. Sepsis-associated acute kidney injury: consensus report of the 28th acute disease quality initiative workgroup. Nat Rev Nephrol. 2023;19(6):401–17.
28. Song MJ, Jang Y, Legrand M, Park S, Ko R, Suh GY, Oh DK, Lee SY, Park MH, Lim CM, et al. Epidemiology of sepsis-associated acute kidney injury in critically ill patients: a multicenter, prospective, observational cohort study in South Korea. Crit Care. 2024;28(1):383.
29. Kuwabara S, Goggins E, Okusa MD. The pathophysiology of sepsis-associated AKI. Clin J Am Soc Nephrol. 2022;17(7):1050–69.
30. Legrand M, Bagshaw SM, Bhatraju PK, Bihorac A, Caniglia E, Khanna AK, Kellum JA, Koyner J, Harhay MO, Zampieri FG, et al. Sepsis-associated acute kidney injury: recent advances in enrichment strategies, sub-phenotyping and clinical trials. Crit Care. 2024;28(1):92.
31. Xu J, Li J, Li Y, Shi X, Zhu H, Chen L. Multidimensional landscape of SA-AKI revealed by integrated proteomics and metabolomics analysis. Biomolecules. 2023;13(9):1329.
32. Klein Haneveld MJ, Lemmen CHC, Brunekreef TE, Bijl M, Jansen AJG, de Leeuw K, Spierings J, Limper M. Erratum to: diagnosis and treatment of patients with antiphospholipid syndrome: a mixed-method evaluation of care in The Netherlands. Rheumatol Adv Pract. 2021;5(2):028.
33. Silpa-archa S, Ruamviboonsuk P. Diabetic retinopathy: current treatment and thailand perspective. J Med Assoc Thai. 2017;100(Suppl 1):S136-147.
34. Wang T, Huang Y, Zhang X, Zhang Y, Zhang X. Advances in metabolic reprogramming of renal tubular epithelial cells in sepsis-associated acute kidney injury. Front Physiol. 2024;15:1329644.
35. Chen L, Huang L, Gu Y, Cang W, Sun P, Xiang Y. Lactate-lactylation hands between metabolic reprogramming and immunosuppression. Int J Mol Sci 2022;23(19).
36. Zhang W, Wang G, Xu ZG, Tu H, Hu F, Dai J, Chang Y, Chen Y, Lu Y, Zeng H, et al. Lactate is a natural suppressor of RLR signaling by targeting MAVS. Cell. 2019;178(1):176-189.e115.
37. Qiao J, Tan Y, Liu H, Yang B, Zhang Q, Liu Q, Sun W, Li Z, Wang Q, Feng W, et al. Histone H3K18 and Ezrin lactylation promote renal dysfunction in sepsis-associated acute kidney injury. Adv Sci. 2024;11(28):e2307216.
38. Uchida T, Yamada M, Inoue D, Kojima T, Yoshikawa N, Suda S, Kamohara H, Oda T. Involvement of innate immune system in the pathogenesis of sepsis-associated acute kidney injury. Int J Mol Sci 2023;24(15).
39. Reimann H, Stopper H, Polak T, Lauer M, Herrmann MJ, Deckert J, Hintzsche H. Micronucleus frequency in buccal mucosa cells of patients with neurodegenerative diseases. Sci Rep. 2020;10(1):22196.
40. Chen X, Xiong X, Cui D, Yang F, Wei D, Li H, Shu J, Bi Y, Dai X, Gong L, et al. DEPTOR is an in vivo tumor suppressor that inhibits prostate tumorigenesis via the inactivation of mTORC1/2 signals. Oncogene. 2020;39(7):1557–71.

Publisher's Note Springer Nature remains neutral with regard to jurisdictional claims in published maps and institutional affiliations.